

NASA/CR—2000-210035



Advanced Propulsion System Studies in High Speed Research

Charles L. Zola
University of Toledo, Toledo, Ohio

April 2000

The NASA STI Program Office . . . in Profile

Since its founding, NASA has been dedicated to the advancement of aeronautics and space science. The NASA Scientific and Technical Information (STI) Program Office plays a key part in helping NASA maintain this important role.

The NASA STI Program Office is operated by Langley Research Center, the Lead Center for NASA's scientific and technical information. The NASA STI Program Office provides access to the NASA STI Database, the largest collection of aeronautical and space science STI in the world. The Program Office is also NASA's institutional mechanism for disseminating the results of its research and development activities. These results are published by NASA in the NASA STI Report Series, which includes the following report types:

- **TECHNICAL PUBLICATION.** Reports of completed research or a major significant phase of research that present the results of NASA programs and include extensive data or theoretical analysis. Includes compilations of significant scientific and technical data and information deemed to be of continuing reference value. NASA's counterpart of peer-reviewed formal professional papers but has less stringent limitations on manuscript length and extent of graphic presentations.
- **TECHNICAL MEMORANDUM.** Scientific and technical findings that are preliminary or of specialized interest, e.g., quick release reports, working papers, and bibliographies that contain minimal annotation. Does not contain extensive analysis.
- **CONTRACTOR REPORT.** Scientific and technical findings by NASA-sponsored contractors and grantees.

- **CONFERENCE PUBLICATION.** Collected papers from scientific and technical conferences, symposia, seminars, or other meetings sponsored or cosponsored by NASA.
- **SPECIAL PUBLICATION.** Scientific, technical, or historical information from NASA programs, projects, and missions, often concerned with subjects having substantial public interest.
- **TECHNICAL TRANSLATION.** English-language translations of foreign scientific and technical material pertinent to NASA's mission.

Specialized services that complement the STI Program Office's diverse offerings include creating custom thesauri, building customized data bases, organizing and publishing research results . . . even providing videos.

For more information about the NASA STI Program Office, see the following:

- Access the NASA STI Program Home Page at <http://www.sti.nasa.gov>
- E-mail your question via the Internet to help@sti.nasa.gov
- Fax your question to the NASA Access Help Desk at (301) 621-0134
- Telephone the NASA Access Help Desk at (301) 621-0390
- Write to:
NASA Access Help Desk
NASA Center for Aerospace Information
7121 Standard Drive
Hanover, MD 21076

NASA/CR—2000-210035



Advanced Propulsion System Studies in High Speed Research

Charles L. Zola
University of Toledo, Toledo, Ohio

Prepared under Cooperative Agreement NCC3-193

National Aeronautics and
Space Administration

Glenn Research Center

April 2000

This report is a formal draft or working paper, intended to solicit comments and ideas from a technical peer group.

This report contains preliminary findings, subject to revision as analysis proceeds.

Trade names or manufacturers' names are used in this report for identification only. This usage does not constitute an official endorsement, either expressed or implied, by the National Aeronautics and Space Administration.

Available from

NASA Center for Aerospace Information
7121 Standard Drive
Hanover, MD 21076
Price Code: A03

National Technical Information Service
5285 Port Royal Road
Springfield, VA 22100
Price Code: A03

ADVANCED PROPULSION SYSTEM STUDIES IN HIGH SPEED RESEARCH

Charles L. Zola*
University of Toledo
Toledo, Ohio 43606

SUMMARY

Propulsion for acceptable supersonic passenger transport aircraft is primarily impacted by the very high jet noise characteristics of otherwise attractive engines. The mixed flow turbofan, when equipped with a special ejector nozzle seems to be the best candidate engine for this task of combining low jet noise with acceptable flight performance. Design, performance, and operation aspects of mixed flow turbofans are discussed. If the special silencing nozzle is too large, too heavy, or not as effective as expected, alternative concepts in mixed flow engines should be examined. Presented herein is a brief summary of efforts performed under cooperative agreement NCC3-193. Three alternative engine concepts, conceived during this study effort, are herein presented and their limitations and potentials are described. These three concepts intentionally avoid the use of special silencing nozzles and achieve low jet noise by airflow augmentation of the engine cycle.

INTRODUCTION

The potential for economically viable and environmentally acceptable high speed transport aircraft depends on the proper evaluation, selection, and integration of the most desirable propulsion system. Advanced propulsion concepts are under consideration by both government and industry under in-house and contracted efforts of the NASA-HSR program. Evaluation of these and other propulsion concepts must be given the highest priority and emphasis to clarify and strengthen program plans for research and

*Research Associate.

technology development. Particular emphasis must be given to aircraft noise reduction and low emission combustor development.

This report is a brief summary of efforts performed under cooperative agreement NCC3-193. General aspects of turbofan engine performance are discussed in order to highlight the advantages and disadvantages of such engines for supersonic transport propulsion. This effort also included the conceiving of new or alternate candidate propulsion concepts which could be capable of low noise takeoff without the use of special mixer-ejector nozzles. These concepts are described and their performance potential is discussed. An appendix is included for an analysis and discussion of mixer effectiveness which led to an improvement in engine cycle analysis computer coding.

Turbofan Engines

Engine cycle definition.-Schematics of two of the candidate engine concepts in current high speed research(HSR) are shown in figure 1. The TBE engine is a turbojet but is included in the figure because it was an early candidate for HSR due to its simplicity (1 spool) , high thrust/weight ratio, and relatively smaller size. However mission/system analysts have found that the jet noise reduction needs for the TBE force too great a compromise with engine performance and weight when compared with the mixed flow turbofan (MFTF). The MFTF has emerged as the probably-best candidate propulsion concept for HSR , especially when integrated with the advanced mixer-ejector nozzle for suppression of takeoff jet noise.

The MFTF has two "spools" or shafts with paired compressors and turbines. The low pressure compressor, "fan", is designed to mismatch the airflow capability of the high pressure compressor, HPC, such that the excess airflow is "bypassed" around the so-called engine "core" via the bypass duct . The bypass flow and the core engine turbine exhaust flow are then mixed prior to the engine nozzle. This bypass capability and the limited de-coupling of the two engine spools can result in lower nozzle jet velocity and more flexibility in reduced power operation . The MFTF has the advantage, relative to the turbojet, of lower fuel consumption at full or reduced power without overly compromising engine weight and thrust. In fact, it can be said that the slightly lower jet velocity of a MFTF , compared with a turbojet, improves propulsive efficiency and overall efficiency of the engine by decreasing specific fuel consumption, SFC. Overall efficiency is directly proportional to flight speed , inversely proportional to SFC , and is not effected by engine thrust. Hence, as long as the thrust output of the engine is sufficient to climb, accelerate, and cruise the aircraft, the lowest possible SFC should be sought. This implies that a lower jet velocity engine , such as a turbofan, will be preferred.

Mixer effectiveness.- The mixer of the MFTF is sketched in figure 2, where the bypass duct airflow and the core engine turbine exit airflow must be brought together at equal static pressures, even if their total pressures differ. This is done by varying the flow areas of each mixer entrance to cause different Mach numbers (different static/total pressure ratios) to accommodate total pressure differences. A total pressure difference of 50% can be accepted in this way without too large a subsonic Mach number in either stream. However, it must be assumed that the two flows cannot mix "ideally" with all the thrust advantages that ideal mixing would yield. Hence, a mixer "effectiveness" must be assumed. The effectiveness, 100% or less, defines the amount of gross thrust gain over separate, un-mixed flow (zero effectiveness) relative to fully mixed flows (100% effectiveness). Mixer effectiveness was seen to be an important and necessary addition to our engine cycle analysis. Therefore, as part of this effort, a simplified model of the process was analyzed and programmed for immediate use in the NEPP engine cycle computer code. The details of mixer effectiveness analysis and other background are presented herein in Appendix A. The mixer effectiveness of high bypass and/or forced (i.e. vanes and chutes) mixers in current studies is assumed to be 80%. However, very low bypass and/or unforced mixers are currently assumed to provide only 40% effectiveness.

MFTF cruise performance.- The relation between MFTF design parameters and cruise performance is shown in figure 3. In the figure, operation of the MFTF cycle is specified at a typical HSR cruise condition of Mach 2.4 and an altitude of 60000 ft. A bypass ratio (BPR), turbine rotor inlet temperature (RIT), and maximum compressor outlet temperature (T3) are used in defining the cycle. The pressure ratio of the "fan" is determined by the requirement that the flows mix at equal static pressures. For this example, the engines are forced to have equal total pressure at the duct and turbine entrances of the mixer. This ratio of total pressures (duct/core) has been called "K" and is another important cycle design parameter and will be discussed later. For now, here in figure 3, K is 1.0 at the cruise condition.

The data in figure 3 assume a maximum T3 of 1760 °R. Cruise BPR is varied from near zero(.01) to .75 . Each point on the figure represents a different MFTF engine. Here, the design RIT is varied from very high(3800 °R) to as low as 3200 °R. Note that the BPR has the most dominant effect on specific thrust, F_n/W_a . Whatever the design value of RIT, design BPR can change the thrust by 50%. On the other hand, changes in SFC and, hence, changes in cruise fuel fraction, are only about 3% over a wide range of BPR. This implies that the HSR aircraft fuel load fraction will not be as sensitive to engine cycle selection as will the thrust produced by the engines for climb, acceleration, and cruise margins. Also shown in figure 3 is an example of the

F_n/W_a and SFC if the limiting T_3 is decreased by 100 °R. In this case, specific thrust is nearly constant, but the impact on SFC is equivalent to a 300 °R change in RIT. Hence, figure 3 shows that limits on T_3 strongly impact SFC, and that the most significant effect of BPR is on thrust.

MFTF fan pressure and bypass ratio.- In figure 4, a range of possible engine designs is shown versus the fan pressure (PRF) at sea level static (sls) conditions. The parameter TTR in the figure is simply a way of expressing the RIT at sls as a value always less than the maximum allowable RIT, since $TTR = \text{MaxRIT}/\text{RIT}$. The BPR shown in the top part of figure 4 is the value at sls, which is always less than the value of BPR at 2.4M by about .15 to .20. Again, the MFTF engines of the figure are designed with a limit value of T_3 , here set at 1660 °R. The engines also must satisfy a secondary constraint such that the ratio of total pressure at the mixer ($K = P_{\text{duct}}/P_{\text{core}}$) be 1.0 or greater. In all cases, K at sls is 1.0 but is allowed to optimize at values above 1.0 for maximum thrust on the flight path up to 2.4M.

Depending on PRF and TTR, the upper part of figure 4 shows the wide range of BPR possibilities between 0 and 1.0. However, at low values of PRF, a limit line of minimum BPR exists such that $K=1.0$ at 2.4M. Note that the BPR can be zero while the PRF varies from 3.6 to 5.0, with appropriate change in TTR. Such cases can be considered two-spool turbojets, although their BPRs increase to about .15 at 2.4M. Lines of constant K , the mixer total pressure ratio at 2.4M, would be almost parallel to lines of constant TTR. In fact, low values of TTR, such as 1.0 to 1.05, are highly undesirable because they correspond to values of K greater than 1.5 at 2.4M. Such engines encounter sonic or near-sonic velocities in their mixers at supersonic flight speeds. For this reason, if an engine with, say, a $BPR=.60$ at sls were desired, the PRF should be 3.0 to 3.4, to avoid high Mach number in the mixer. It can be seen, however, that this range of PRF may compromise the transonic thrust capability of the engine, as shown in the bottom part of figure 4.

Acceleration thrust.- The lower part of figure 4 shows the relative transonic thrust of MFTF engines at equal sls airflow size over the same range of TTR and PRF as in the upper figure. As mentioned before in figure 3, it is the thrust capability of the engine to accelerate and climb the aircraft which is probably the most dominant discriminator, since cruise SFC (and Breguet factor) variations are small once RIT_{max} and T_3 limits are set. The transonic thrust, here chosen at Mach 1.1 and 30000 ft., is a good indicator of the performance differences between various MFTF designs. Transonic thrust varies in direct proportion to other thrusts on the flight path, such as start of climb and top of climb. An obvious feature of the figure is that $BPR=0$, or low BPR along the $K=1$ limit, results in the best transonic thrust at any PRF.

Also note that, at each PRF, the range of transonic thrust is surprisingly small for the range of TTR shown. As stated, the data in figure 4 are for the same engine airflow size. Hence, a thrust margin problem, due to choice of BPR and PRF for other reasons such as takeoff jet velocity, jet noise, or thrust, can be readily solved by a physical size (airflow) change of the engine. A 15% increase in engine size can easily offset any negative effects of choice of PRF, TTR, etc. on transonic thrust capability. This point is stressed because the bare engine weight (at equal airflow size) can decrease by 40% as the bypass ratio of the MFTF is increased from low (about .10) to high (about 1.0).

This analysis of the MFTF has been presented because it is the most likely successful candidate concept for HSR propulsion and should therefore be understood. Also, other concepts to be discussed herein share similar characteristics and considerations as the MFTF and, on parts of their flight path, may even be mixed flow turbofans or two-spool turbojets with identical limits in K, TTR, etc.

INVERTER FLOW VALVE (IFV) ENGINES

IFV turbojet engine.- The possible thrust advantages of two-spool engines that are turbojets or very low BPR have been mentioned. Their drawback is the need for a method or device to decrease takeoff jet noise level. In most HSR engine designs, the low noise - low jet velocity is assumed to be brought about by the attachment of a special ejector nozzle which adds and mixes enough secondary airflow to the engine exhaust to lower the "effective" jet velocity to about 1500 fps. The amount of secondary flow needed varies from 120% for turbojets at high RIT to as low as 30% for MFTF engines at higher BPR, since they already have moderate jet velocity.

As an alternative, in case mixer-ejector nozzles are too heavy, too large, or not as effective as postulated, an engine concept was proposed in which the takeoff airflow is greatly increased to simulate the effect of high BPR. This engine concept would then "convert" to lower airflow while flying at subsonic speeds, and then proceed on the accel/climb path as a two-spool turbojet. Figure 5 shows a schematic of the so-called TJ/IFV engine. The engine sketch is highly simplified to show the relation between the inverter flow valve (IFV) and the other, more usual, engine components. The IFV concept evolved in early studies of flow switching engine concepts in vertical takeoff aircraft. The IFV has also been called an annular inverting valve(AIV), which may be a more descriptive term once its operation is described. The terms IFV and AIV are used interchangeably. Weight and dimension estimates for AIV's were an important part of this effort and involved computer code improvements for engine weight estimates. However, no

highly rigorous methodology for AIV analysis exists that would predict credible weights within, say, 20%.

The IFV, as sketched in figure 5, is best described as two large, matching, drumlike cylinders, each of larger diameter than length. Each drum/cylinder comprises half of the inverter valve. Each cylindrical half is further subdivided into smaller passages, which line up with similar passages in the other cylinder. When the passages of the two cylindrical halves of the IFV are aligned in their "inverter" position, airflow moves through the inner passages of the front half and is diverted to the outer passages of the rear half. Likewise, flow entering the outer passages of the front half emerges from the inner passages of the rear half. One of the two IFV halves is fixed and the other is moveable, allowing it to index by rotation sufficient to re-align the flow passages. when this is done, the IFV does not invert the flows of the inner and outer passages. Hence, the flow paths can be switched from straight through to inversion, depending only on the index position of one IFV half relative to the other. In a six passage IFV as sketched in figure 5, there are twelve segments at valve mid-plane, each taking a 30 degree wedge. This valve would therefore need only a 30 degree indexing movement to invert the flows. Prototypes have been built that accomplished the index movement in about 0.5 seconds.

In the TJ/IFV, the IFV is in straight through flow position for turbojet operation. Airflow entering the low compressor passes on to the high compressor by flowing through the IFV, sensing only a parasitic pressure loss. There is no flow in the outer circumference passages of the valve in turbojet mode. In high-flow operation, the valve is re-indexed to conduct the exit flow of the low compressor out to the bypass duct. Meanwhile, secondary inlets for ambient air are opened in the outer entrance of the front half of the AIV. This secondary inlet airflow is conducted to the inner passages of the rear half of the valve, where it can then enter the high compressor. In effect, the flows have been switched or "inverted" and the engine cycle has been changed from a turbojet to a turbofan. The bypass ratio of the turbofan is the ratio of the front compressor airflow to that of the rear or high compressor. In many cases the effective BPR is about 2.0.

Figure 6 presents a weight assessment and cycle data for the TJ/IFV. The weight of the engine in figure 6 is low by 5 or 10% when compared with more recent estimates of engine company specialists. The design of supersonic engines that make use of devices such as an IFV is a new field with many technology challenges and un-addressed questions. Both engine weight and engine performance estimates can often become hostage to the degree of conservatism employed. Note, however, that the cycle data shown remains representative. The equivalent BPR in high flow is 1.7. The flow of the high

compressor (Wac2) is 438 pps in high flow, whereas it is only 282 pps in low flow turbojet mode. This "swing" in corrected flow of the high compressor is accomplished by an intentional change in corrected speed. Of note is that this change in actual RPM is very small. The peak cycle pressure ratio in turbojet mode is about 21. But in high flow mode, without the contribution of the front compressor, the peak cycle pressure is only about 7. Figure 7 gives another schematic of the TJ/IFV engine, along with several comments to underscore the need to consider such engine cycles for HSR. Of particular significance is the point that Stage IV jet noise limits may be 5dB less than current HSR ground rules. The mixer-ejector nozzles that are currently envisioned may not be able to achieve this new level of noise reduction. It represents an "effective" jet velocity of about 1300 fps.

The TJ/IFV engine concept is prone to certain drawbacks which narrow design choices and may compromise the performance and effective integration of the engine on an aircraft. These challenges are summarized in figures 8 and 9. The apparent advantage of a swing in BPR from 0 to about 2.0, is accompanied by some severe component design requirements and compromises. The total diversion of the front compressor flow causes large, heavy AIV's and extra inlet weight and size for auxiliary intakes. At the same time, the high(rear) compressor is de-supercharged by the flow bypassing the front compressor. In addition, the rear compressor physical size must be large enough to accommodate the high level of corrected flow. The choices in cycle design to meet these flow-matching needs are narrowed, especially when the added requirement that the flows mix at the turbine exit is recognized.

VBSC engine.- The VBSC engine concept grew from the desire to utilize the AIV in an engine for an increase in BPR without de-supercharging the core engine high compressor. Hence the name, variable bypass supercharged core (VBSC), is used for the engine concept sketched in figure 10. The engine use an IFV, but only on the outer, or "bypass", portion of the flow exiting the front compressor (fan). The inner portion of the fan flow is ducted straight through the IFV hub to enter the engine core compressor. This center flow path does not change, regardless of the index position of the IFV. In normal, or low-flow mode, the engine is a moderate BPR turbofan but with the added feature of a high-spool driven rear fan stage. This core-driven rear fan stage helps to increase the total pressure in the bypass duct, suitable to that of a moderate BPR turbofan, when the VBSC is in its low-flow mode. The core driven rear fan stage has been used in other engines and has been seen to provide some benefits such as lower temperature at the LPT entrance due to a shift of work to the HPT, and better thrust at transonic acceleration and top of climb, due to nearly constant BPR on the flight path, unlike the increase of BPR in conventional mixed flow turbofans. In low flow, low BPR mode the outer passages of the IFV are not used in the VBSC.

In high flow mode for the VBSC, the IFV is indexed to direct the outer fan flow to an outer bypass duct., bypassing the core-driven rear fan. Auxiliary inlet flow is taken into the outer passages at the front of the IFV and then directed to the inner outlet of the rear half of the valve to supply the outer portion, or tip, of the core-driven fan stage. This core-driven fan therefore includes a rotating splitter to isolate the flows of its inner and outer portions. This outer flow exits into the bypass duct in both high and low flow modes. However, in high flow mode, the bypass duct flows are mixed with a total pressure difference of less than 50%, to avoid high internal velocity differences. The combined bypass flows are then mixed in the main engine mixer at the core turbine exit. The example in figure 10 is typical, with a BPR change from .60 to 1.13 between low and high flow modes. Since the high flow BPR is not very large, the engine also requires a degree of reduced RIT at critical jet noise measurement points and during takeoff to keep the jet velocity to about 1500 fps. Thus, takeoff thrust of the VBSC is less than its potential.

In figure 11, a typical VBSC installation is sketched and pertinent weight and performance data are shown, Note that the secondary airflow is only 200 pps in the high flow mode, hence a flow increase of only about 30% over the base turbofan of its low flow mode. Although valve weight and auxiliary inlet weight benefit from the lower airflow increment, it appears that the takeoff thrust compromise is too severe for this concept. Other compromises forced on this engine cycle are the pressure ratios of the front fan and the core-driven rear fan. The rear fan is conservatively assigned a maximum PR of 1.8 in the high flow mode, since it is a single stage. This limit forces an upper limit on the PR of the front fan at about 2.8, in order that the outer duct and bypass flows may mix at reasonable subsonic velocities. This upper limit on front fan PR tends to penalize the engine in its low flow mode by forcing the BPR to be higher than might be desired. Hence, the example given in figure 11 has a BPR of .60 in its base engine (low flow) design, although a lower BPR may yield better performance for most of the climb, acceleration, and cruise flight path.

Figure 12 presents a comparison of the VBSC and MFTF engines at nearly equal cruise BPR and airflow. The sea level static (sls) BPR of the MFTF is about .40, and increases to about .55 as the engine climbs to the 2.4M cruise. The mass flow addition (MFA) of the MFTF is shown as .46, representing the pumping effect of its mixer- ejector nozzle. Net airflow is raised from 750 pps to 1100 pps, resulting in a 50000 lb. thrust, even though the effective jet velocity is low enough for Stage III jet noise. For the VBSC, the MFA is .27, representing the 200 pps of airflow induced by the AIV and auxiliary inlets during high flow mode. For low effective jet velocity, this engine must be operated at lower RIT, resulting in a sls thrust of less than

40000 lb. This is a 20% deficit when compared with the MFTF. Total pod weights are quite similar, with the VBSC being 900 lb. lighter. The VBSC weight penalties in the valve, inlet, and bare engine are less than the 3000 lb. weight difference in the nozzles of the two engines. In mission sizing, the higher thrust/weight of the MFTF pod allows down- scaling of the pod, leading to a lower weight aircraft.

FLADED TURBOFAN

MFFLD engine concept. - Figure 13 is a sketch of a mixed flow turbofan with two so-called "Flade" stages on the outer portion of the fan. The MFFLD engine derives from a desire to increase the duct pressure of the VBSC engine discussed earlier. The evolution of the MFFLD concept is outlined in figure 14.

The core- driven fan tip of the VBSC is shown in the upper sketch of figure 14. This fan stage was limited to a PR of 1.8. A higher PR would require two stages of core- driven fan. If, however, the outer portion of the core- driven fan is relocated to the outer tip of the front fan, and made into two stages, it can easily achieve a PR of 3.0. The nacelle diameter at the front fan is not greatly changed since a peripheral flow area was required around the fan for the outer entrance of the AIV in the VBSC.

Once the fan tip is relocated to the outer portion of the fan, it becomes a "fladed" fan. The flade flow can be regulated from zero to full by means of variable inlet guide vanes (IGV's). The weight of these IGV's, and the weight of the flades and their rotating splitter retainers, etc., add significantly to the weight of the front fan. However, flow switching is no longer needed, hence the valve is removed. The engine still retains a high- and low- flow characteristic, but this is accomplished by the IGV's. The MFFLD concept at the bottom of figure 14 called for two fladed fan stages. It was later found that three fan stages would be preferable for higher PR in the base fan. Therefore the current MFFLD engine corresponds more closely to the schematic sketched in figure 13.

The emphasis of the MFFLD concept is on flow mixing in two areas of the engine, a single exhaust nozzle, high airflow- low jet velocity (V_j) operation at takeoff and subsonic flight, and conventional MFTF operation during accel, climb, and supersonic cruise. Reduced RIT is also utilized to keep V_j low (~1700 fps) in the airport vicinity and further cutback of RIT is employed at critical noise measurement points for a V_j of about 1475 fps. The cycle parameters are chosen to avoid high Mach mixing in the outer ducts during high flow and in the main mixer at the engine rear. No special acoustic shield nozzles or flows are incorporated.

Figure 15 shows pertinent data for a typical MFFLD engine installation. The base MFTF cycle has a BPR of .40 at 2.4M and would have a sls BPR of about .25 if the flades were not used. But, with the extra load of the flowing flade stages and the reduction of RIT for a V_j of 1700 fps, the BPR drops to .10. Installed cruise thrust and SFC are essentially the same as the base engine MFTF. Unlike the VBSC, the MFFLD has no engine weight increment for an AIV and a core-driven fan stage. However, the engine weight data shows a fan of 4125 lb. (about +50% heavier than a normal fan) , due to the IGV's and fladed stages. Other, less obvious, weight increments, such as ducting and bypass duct mixer, also add to the base engine weight.

Preliminary estimates have been made for potential relative takeoff gross weight (TOGW) of a supersonic transport integrated with the propulsion systems mentioned in this summary. Figure 16 presents relative TOGW data for mission- sized aircraft as a function of jet noise suppression. This figure and the data in it must be considered as very preliminary. It is meant to be only representative of the relative status of these propulsion system applications and can change as new technology constraints (bad or good) are encountered and incorporated.

The TJ/IFV, VBSC, and MFFLD are shown on the ordinate because they are assumed to require no suppression for Stage III jet noise. However, curves are shown for the TBE and MFTF indicating different values of TOGW depending on noise suppression. The TBE curve results from decreasing RIT at takeoff to decrease the need for jet noise suppression. It is apparent that the need for silencing the TBE can be decreased (with decreased takeoff F_n/W_a), but at a high cost in installed engine size, leading to increased TOGW. The MFTF curve is similar, but in this case the BPR of the engine at takeoff is increased from .10 to 1.0 to decrease the un-suppressed jet velocity. Again, this decreases F_n/W_a at takeoff and , as pointed out earlier in this report, throughout the flight, calling for increased engine size and increased TOGW. The highest point shown on the MFTF curve illustrates the combination of BPR=1.0 and lower takeoff RIT. This point indicates that different unique combinations of takeoff RIT and BPR would result in about the same curve of TOGW versus noise suppression requirement for the MFTF.

The TJ/IFV data point at about 1.12 relative TOGW is the highest of the dual- mode, high/low airflow concepts. However, less pessimistic engine weight and performance estimates have indicated that a relative TOGW of 1.05 is feasible. At this time it appears that the better thrust/pod weight of the MFFLD places it at a slightly lower value of TOGW relative to the VBSC. However, these engine concepts are also subject to the technology status, engine weight, and performance vagaries noted for the TJ/IFV. It is

expected that their relative TOGW results may vary by, at least, plus or minus 5%.

CONCLUDING REMARKS

Different features of proposed propulsion concepts for the supersonic transport have been described and their individual technology challenge areas have been reviewed. The superior status of the MFTF engine with mixer- ejector nozzle has been recognized, as well as the background reasons for its desirability. Other alternative concepts have also been presented in which the emphasis is on high- airflow, dual mode engine cycles rather than nozzle suppression of jet noise. The three alternative concepts discussed herein each present technology opportunities in areas that are not well-defined. It should be clear that these alternative ideas depend on weight and performance predictions for key engine components that have not been thoroughly studied. As stated earlier, the pursuit of un-conventional solutions to a problem can often become hostage to the degree of conservatism employed before definitive knowledge exists. It is possible that alternative concepts would provide acceptable results, but it is highly likely that their performance potential will be less promising than that of the MFTF with mixer- ejector nozzle.

HSR CANDIDATE PROPULSION CONCEPTS

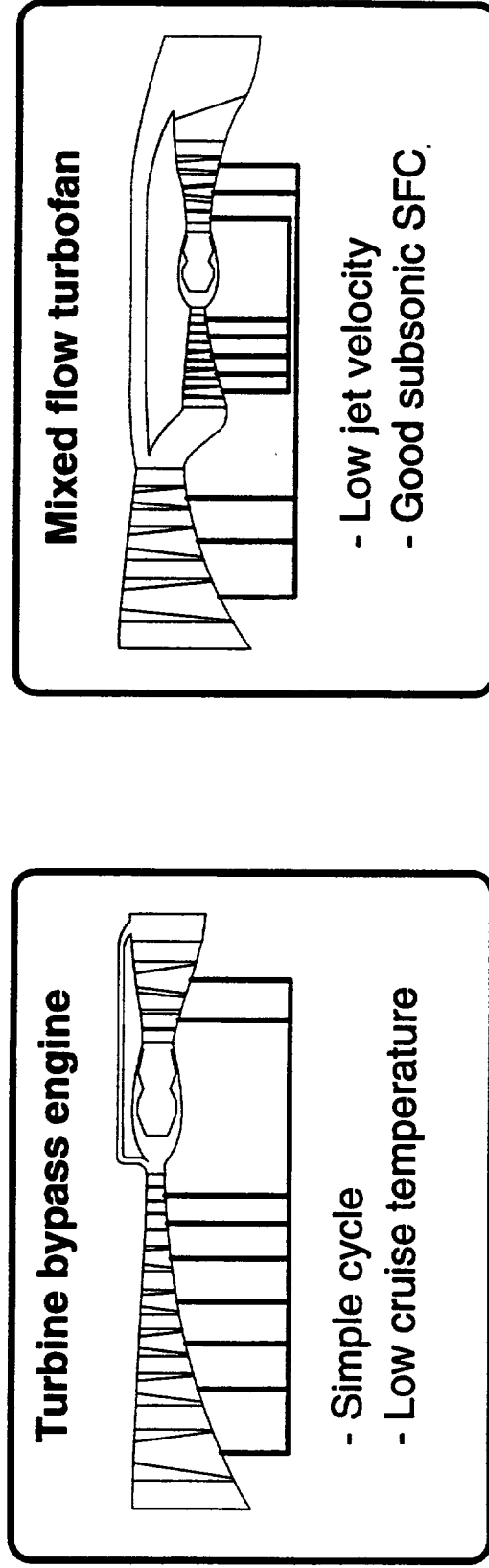


Figure 1

MIXER EFFECTIVENESS ISSUE
AFT END OF TYPICAL MIXED FLOW TURBOFAN
THE NOZZLE FLOW MAY NOT BE TOTALLY MIXED

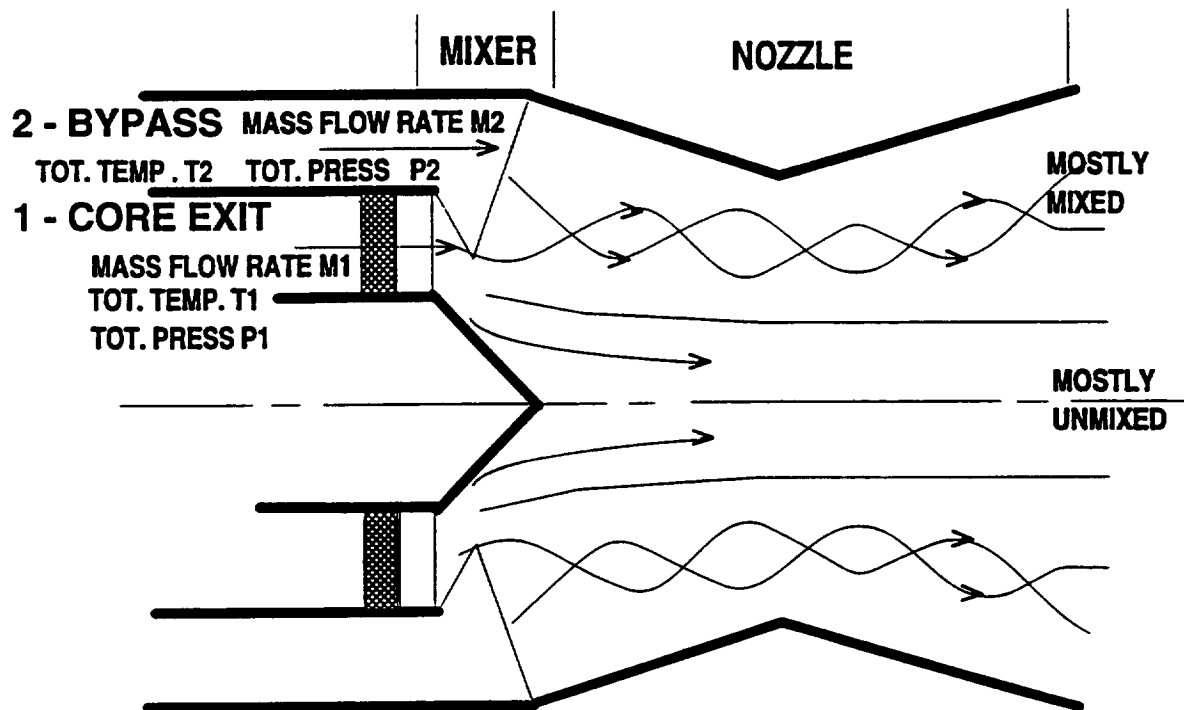


Figure 2

I-H HSR PROPULSION ASSESSMENT

EFFECT OF RIT AND BPR ON PERFORMANCE

DRY TURBOFANS AT DESIGN POINT $h=60000$ ft, $MACH=2.4$
OPR DETERMINED BY T3 SPECIFIED AS $1760^{\circ}R$

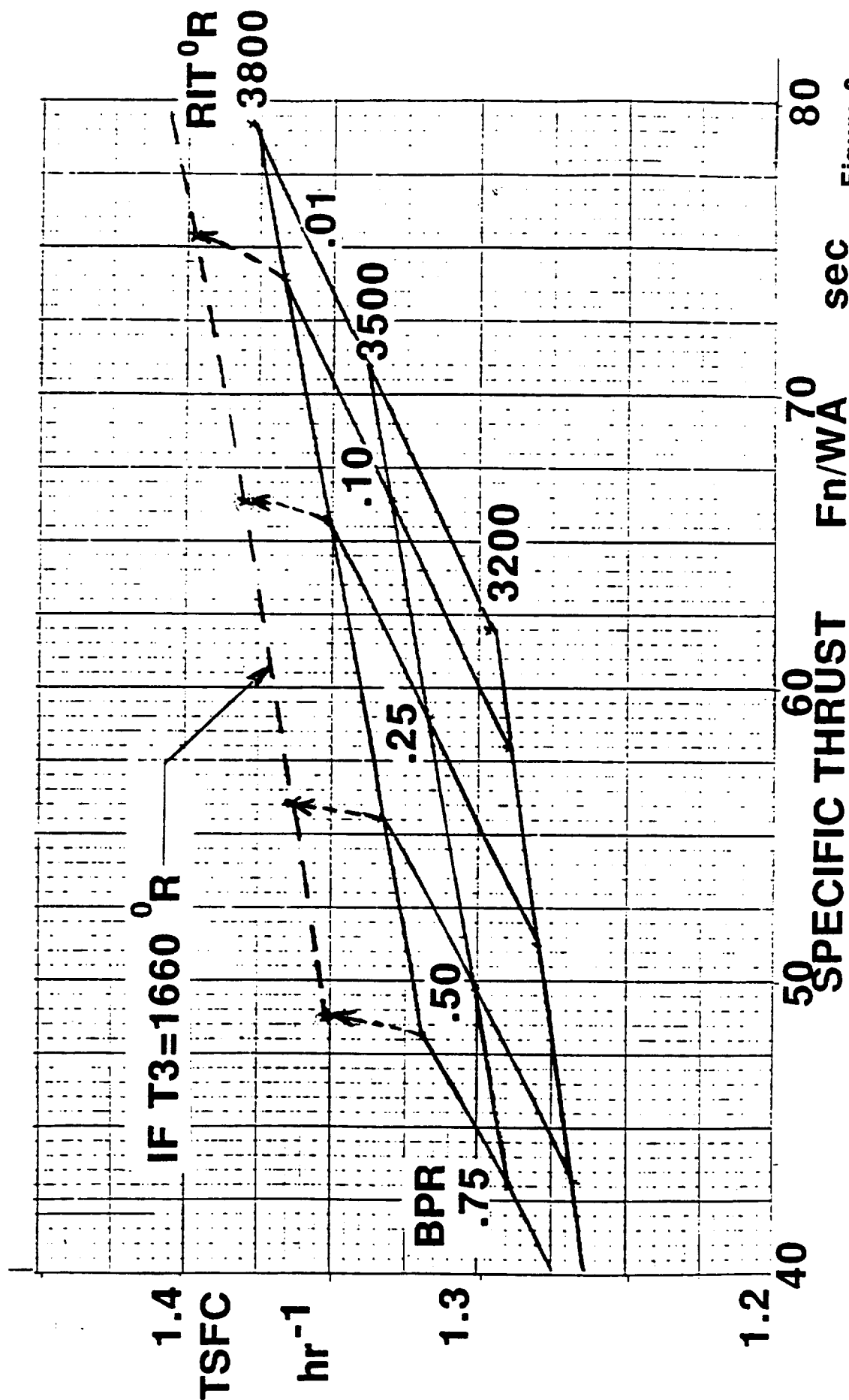


Figure 3

MIXED FLOW TURBOFANS

BPR FPR and THRUST

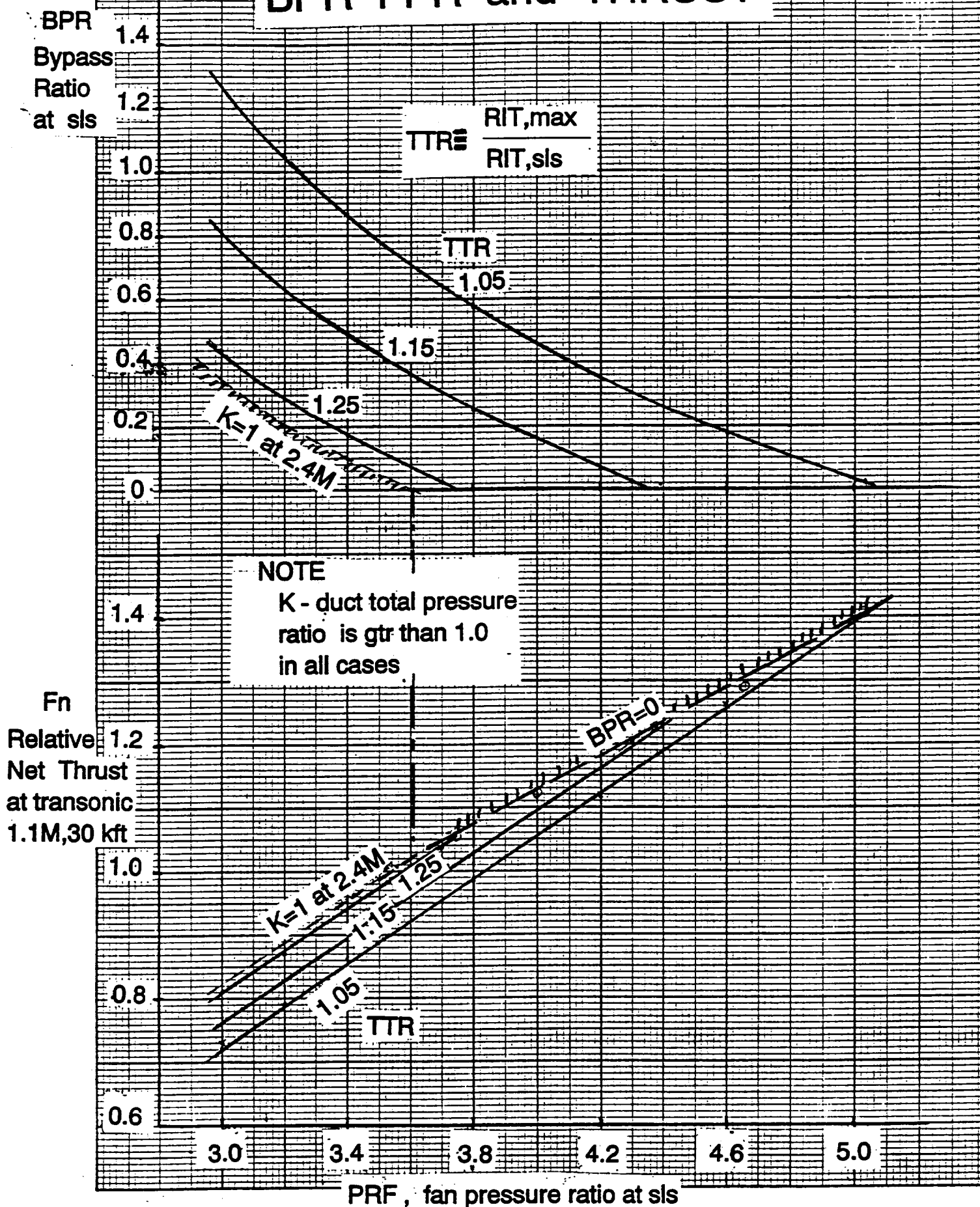
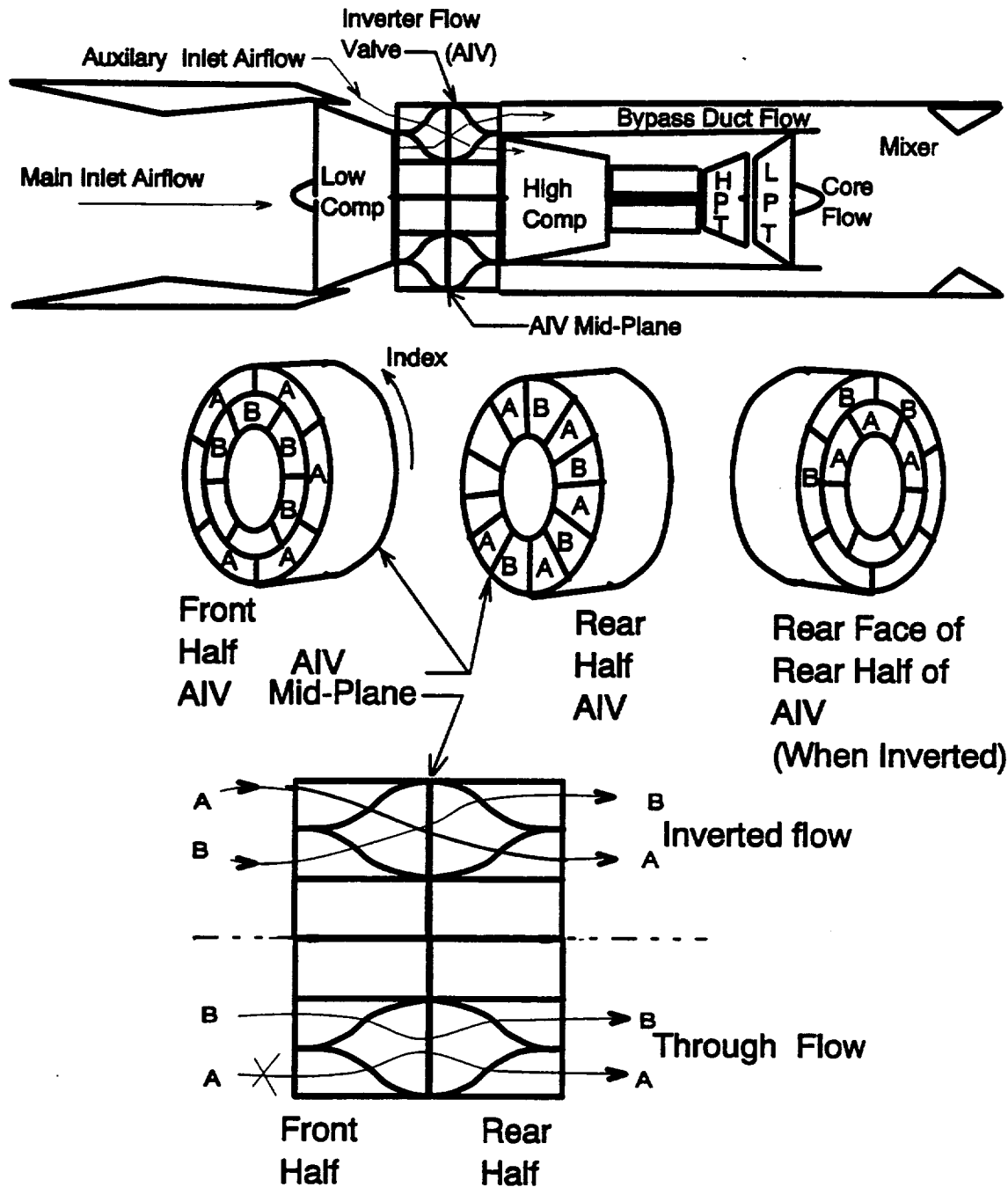


Figure 4

Turbojet/Inverter Flow Valve Engine (TJ/IFV)

Two-Spool Turbojet in Low-Flow Mode Turbofan in High-Flow Mode



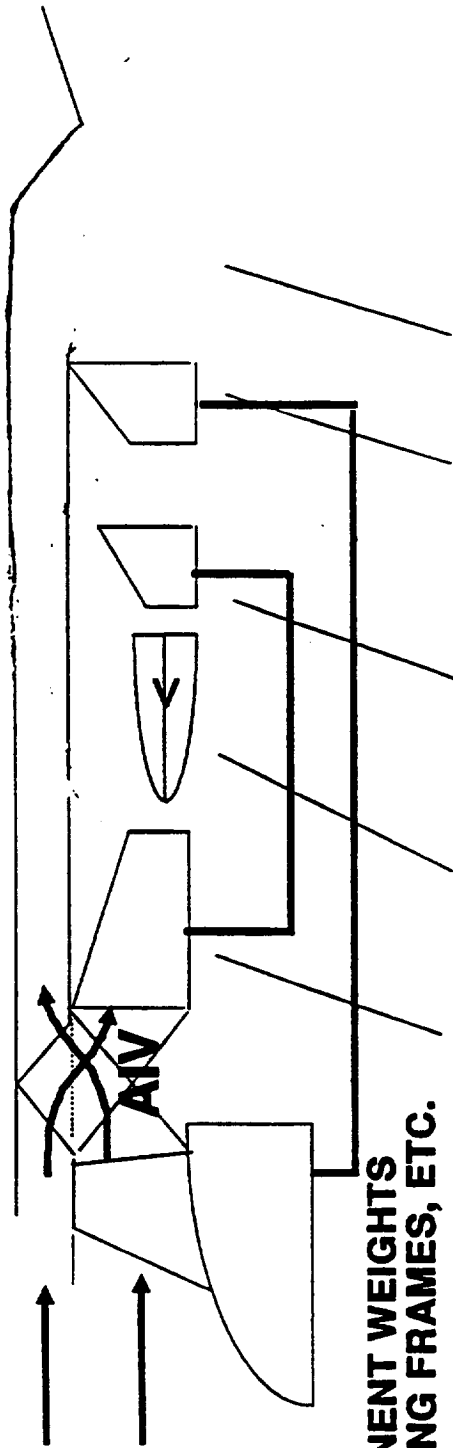
Inverted Flow - Flow Entering A (Outer-Front), Passes Thru Segment A at Mid-Plane, Exits At Inner-Rear. Flow Entering B (Inner-Front) Exits At Outer-Rear Passages.

Through Flow - No Flow In Passages A. Flow entering B (Inner-Front) Exits At Inner Rear.

Figure 5

TJ/IFV

Typical Engine Weight and Performance Data



COMPONENT WEIGHTS
INCLUDING FRAMES, ETC.

FRNT COMPRSR	INVRTR VALVE	REAR COMPRSR	BURNR	HPT	LPT	MXR	SHAFTS	MISC	TOTAL
1000	1000	1300	800	1000	2200	400	500	500	8700

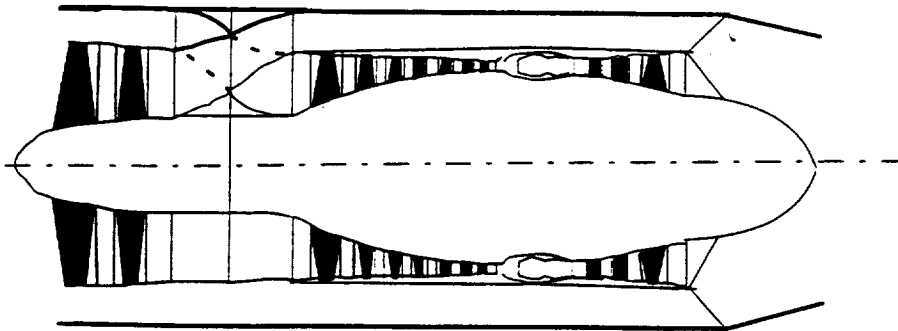
(700 lb/s Ref Flow Size)

PERFORMANCE

MODE	ALT	MACH	WAC1	PR1	NC1	WAC2	PR2	NC2	PRIM VJ	SEC VJ	NET THRUST	EQUIV BPR
HI-FLO	0	0	700	3.16	1.00	438	6.81	1.000	1450	1450	47460	1.70
LO-FLO	0	0	700	3.16	1.00	282	3.67	0.829	2858	--	59860	--
HI-FLO	35K	0.9	700	3.16	1.00	438	6.88	1.000			15347	1.70
LO-FLO	35K	0.9	700	3.16	1.00	282	3.82	0.830			23097	
LO-FLO	35K	1.1	700	3.16	1.00	282	3.74	0.830			27599	
LO-FLO	60K	2.4	700	3.16	1.00	281	3.36	0.827			34236 (MAX)	

Figure 6

TJ/IFV



WHY CONSIDER IFV ENGINES ?

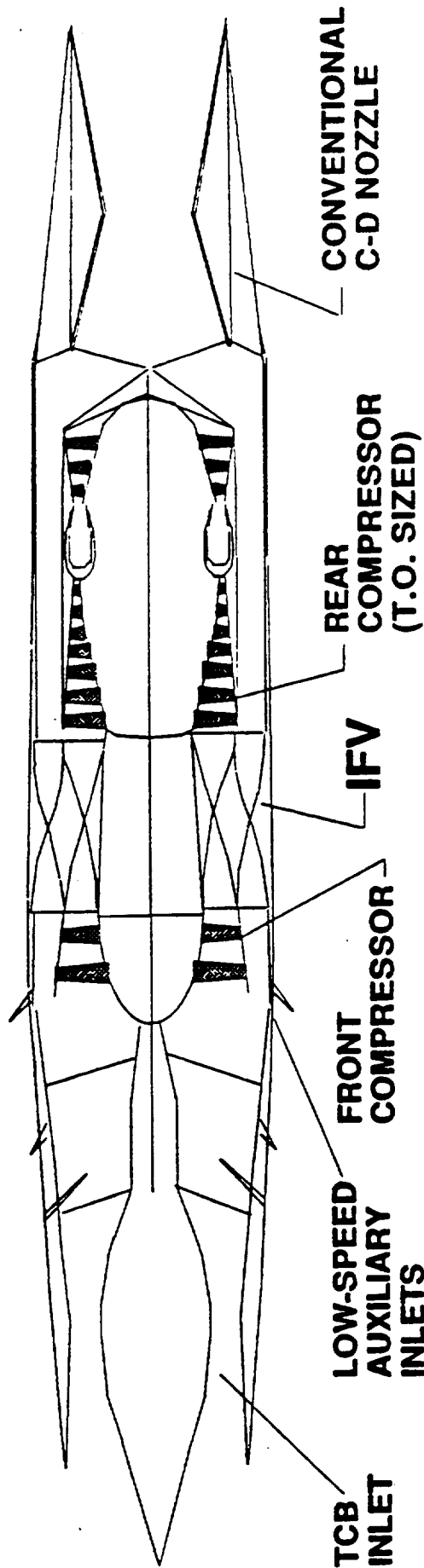
- *Jet Noise $\longrightarrow V_j/g = F_n/W_a$*
- *Stage III Noise Needs $V_j \sim 1500$ fps*
 - *Therefore $F_n/W_a \sim 46.6$*
- *Challenge is to do this with the least investment in propulsion hardware*
 - *Ejector Nozzles, Increase W_a , Decrease V_j*
 - *IFV Concepts for flow switching, Hi-Bypass, Low V_j*
- *Stage IV Noise Level May Require 5 dB less*
 - *$V_j \sim 1300$ fps*
 - *$F_n/W_a \sim 40.4$*

Figure 7

TJ/IFV

TWO-SPOOL TURBOJET W/INVERTER FLOW VALVE

STATUS



Meets Stage III Noise without a Suppressor Nozzle, BUT:

- | | | | |
|---|---|----------------------------|----------|
| Penalties Relative
to MFTF at
50000 lb Fn | { | 1. Heavy | +3000 lb |
| | | 2. Large | +12% L,D |
| | | 3. Less Efficient | + 6% SFC |
| | | 4. High Inlet Aux. Airflow | |

Result is a 6% or Greater TOGW Disadvantage Relative to the Mixed Flow Turbofan With Mixer /Ejector Nozzle

Figure 8

TJ / IFV Engine Characteristics

50,000 lb. Takeoff Thrust Class

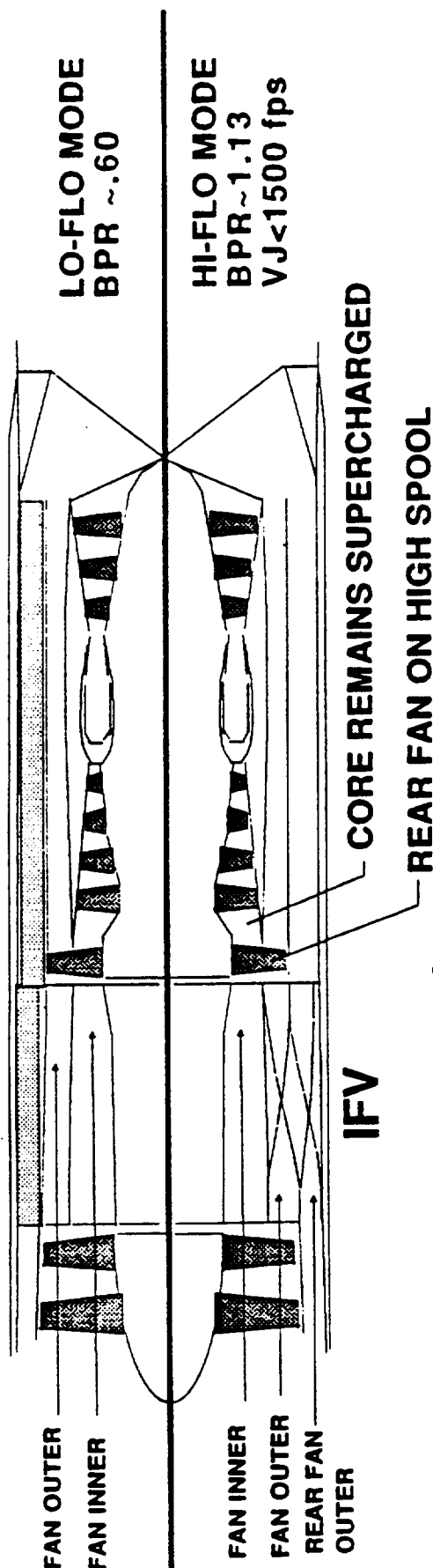
1. De-supercharged core in high flow mode (front compressor removed)
 - Increased weight (3000 lb.)
 - Low thrust, low cycle pressure core
2. Added IFV component
 - 900 lb. IFV weight
 - 950 lb. auxiliary inlet weight
 - 4% cruise ΔP (+1% ΔSFC)
3. Permits conventional unsuppressed nozzle (instead of treated M-E nozzle)
 - 2000 lb. weight savings
 - 0.4% better cruise C_{fg} (-1.1% SFC)
4. IL cruise cycle about 6% higher SFC than a MFTF

Figure 9

VBSC

VARIABLE BYPASS SUPERCHARGED CORE

GENERAL FEATURES



Hi-Flo and Lo-Flo

- Turbofan with core supercharged in either mode
- Reduced size and pressure ratio of core compressor

Lo-Flo

- Outer fan flow directly to rear fan outer
- Inner fan flow path directly to rear fan inner
- Mixed flow turbofan, cruise SFC better than TJ/IFV
- Valve pressure losses on only ~half of engine flow

Hi-Flo

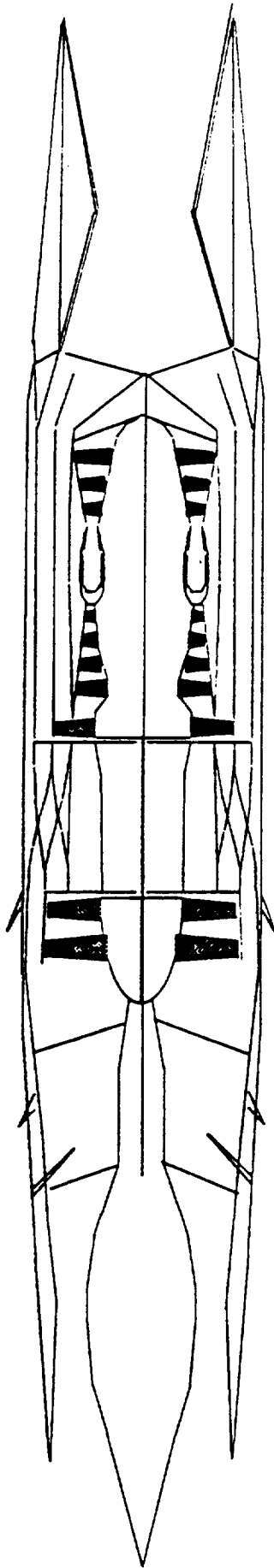
- Front fan outer diverted to outer bypass duct
- Rear fan outer supplied by inlet through IFV
- High bypass, low V_J operation
- Less aux. inlet flow relative to TJ/IFV
- Lower engine weight/ airflow than TJ/IFV

Figure 10

VBSC

VARIABLE BYPASS SUPERCHARGED CORE

PROPULSION POD



POD

TOTAL WEIGHT	16805 lb
LENGTH	39 ft
MAX DIA.	75 in
INLET	3975 lb
VALVE	700 lb
ENGINE +ACCS	8250 lb
C-D NOZZLE	2180 lb
MISC POD	1700 lb

160 in
40 in
185 in
125 in

ENGINE

TAKEOFF - +18F DAY

WAC primary	750 lb/s
WAC secondary	200 lb/s
Equiv BPR	1.13
Fn	39670 lb
Vj Ideal	1480 fps

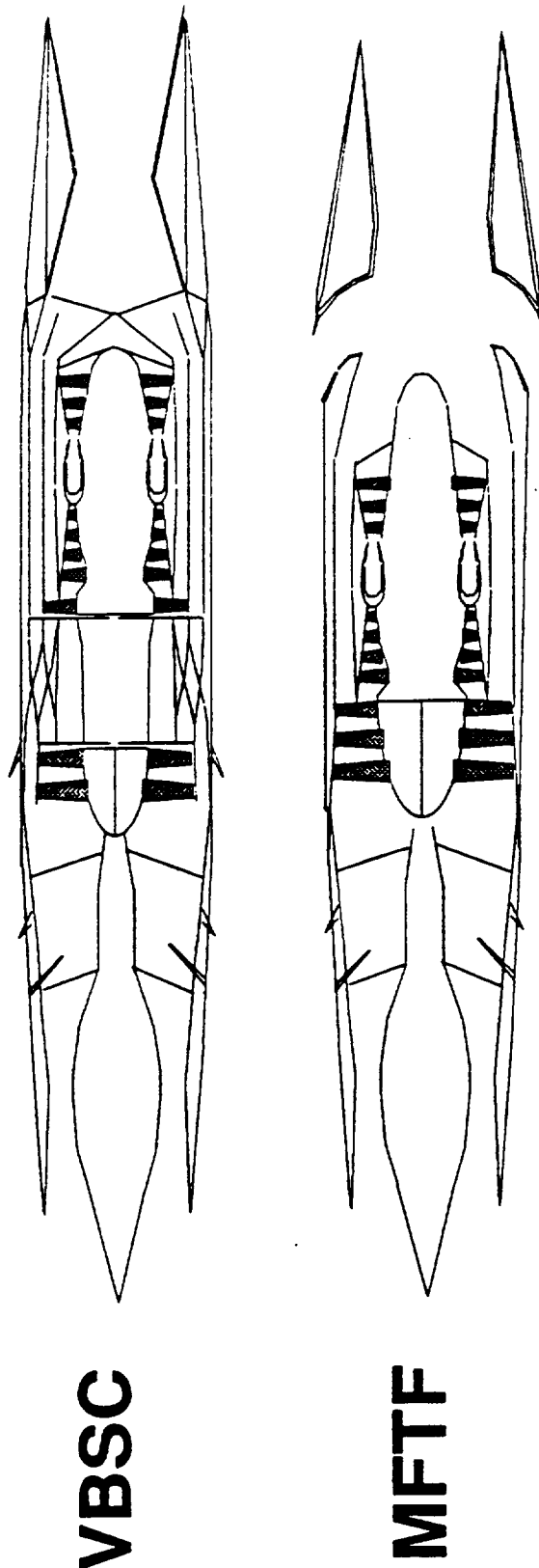
CRUISE 2.4M, 60 Kft

WAC	500 lb/s
BPR	0.60
Fn installed	15845 lb
SFC installed	1.31

Figure 11

VBSC & MFTF

PROPULSION PODS COMPARED



VBSC

BPR	0.60
WAC primary	750 lb/s
WAC noz exit	950 lb/s
MFA	.27
Fn sls	39600 lb
TOTAL WEIGHT	16805 lb
INLET	3975 lb
VALVE	700 lb
ENGINE +ACCS	8250 lb
C-D NOZZLE	2180 lb
MISC POD	1700 lb

MFTF

BPR	0.55
WAC fan	750 lb/s
WAC noz exit	1100 lb/s
MFA	.46
Fn sls	50000 lb
TOTAL WEIGHT	17700 lb
INLET	3500 lb
--	
ENGINE + ACCS	7533 lb
MX/EJ NOZZL	5030 lb
MISC POD	1637 lb

Figure 12

MXD FLOW / Dbl.FLADE MFFLD

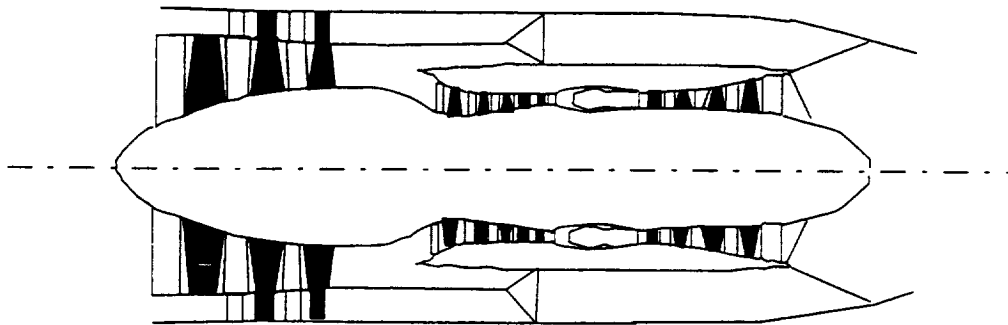
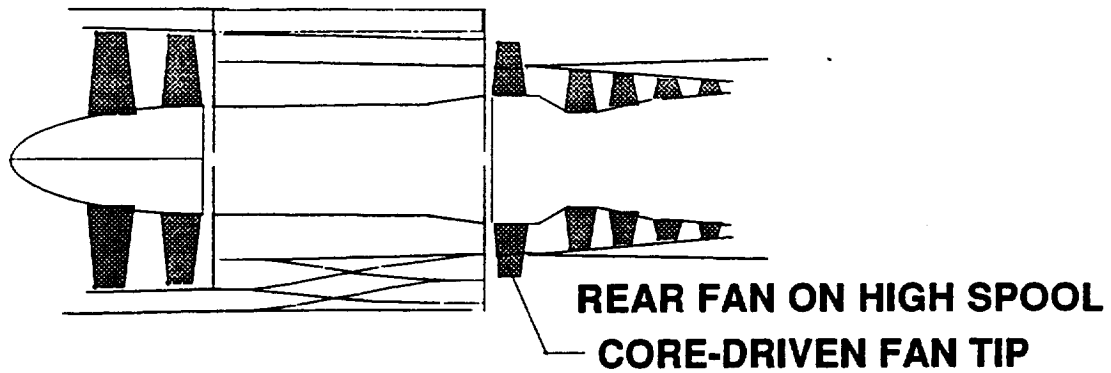


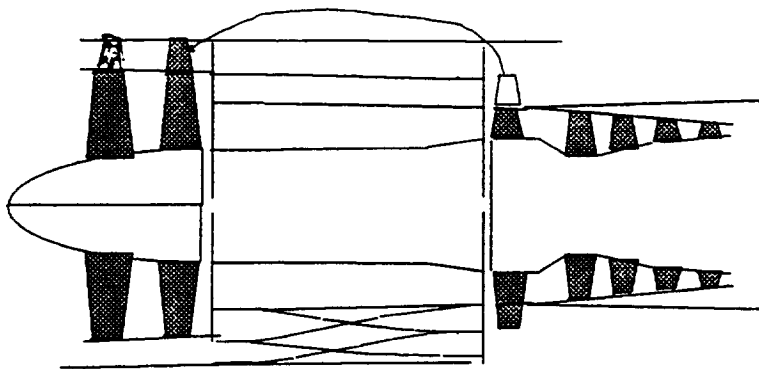
Figure 13

MFFLD CONCEPT EVOLUTION

VBSC



RELOCATE FAN TIP TO OUTER OF FRONT FAN (FLADE)



MFFLD

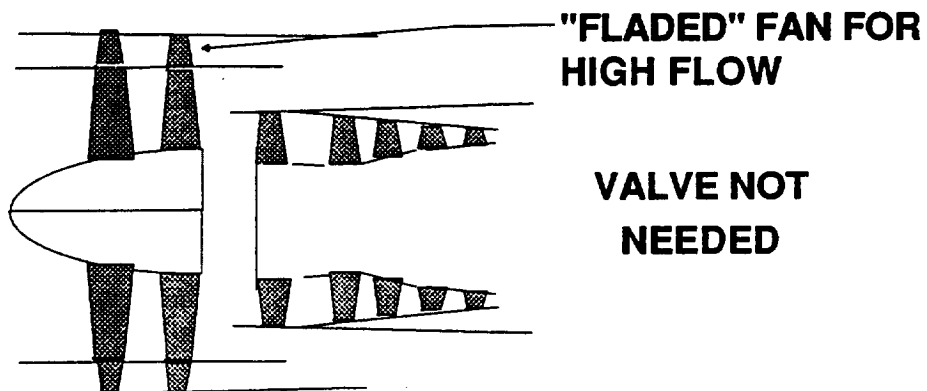
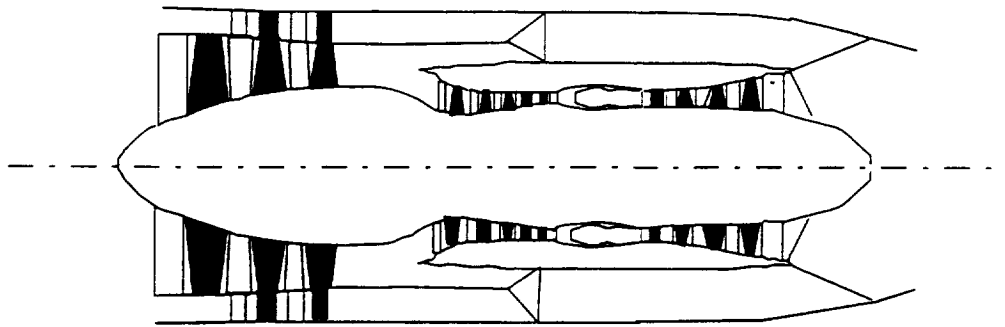


Figure 14

MXD FLOW / Dbl.FLADE MFFLD



S.L.S. +18F DAY - HIGH FLOW - WAC_{tot} = 1000 pps

PR flade	3.0	Wac,flade	350 pps
PR fan	3.8	Wac,fan	650 pps
PR comp	5.5	Inner BPR	0.10
Thrust sls	48000 lb at V _j =1700 fps		
Thrust 0.3M	, 30000 lb at V _j =1475 fps (Noise Cutback)		

Cruise 2.4M at 60000 ft . (Installed)

Wac,tot	455 pps
BPR	0.40
Thrust	15580 lb
SFC	1.33

Propulsion Pod (Nacelle)

Bare Engine + Accs	10375
Fladed Fan	4125
Core Eng	5300
C & A	950
Inlet	3625
Nozzle	2700
Misc. Pod	2300
Total	19000 lb

Figure 15

RELATIVE MISSION - SIZED AIRCRAFT AND NOISE SUPPRESSION

Mach 2.4, 5000 n.mi. Range

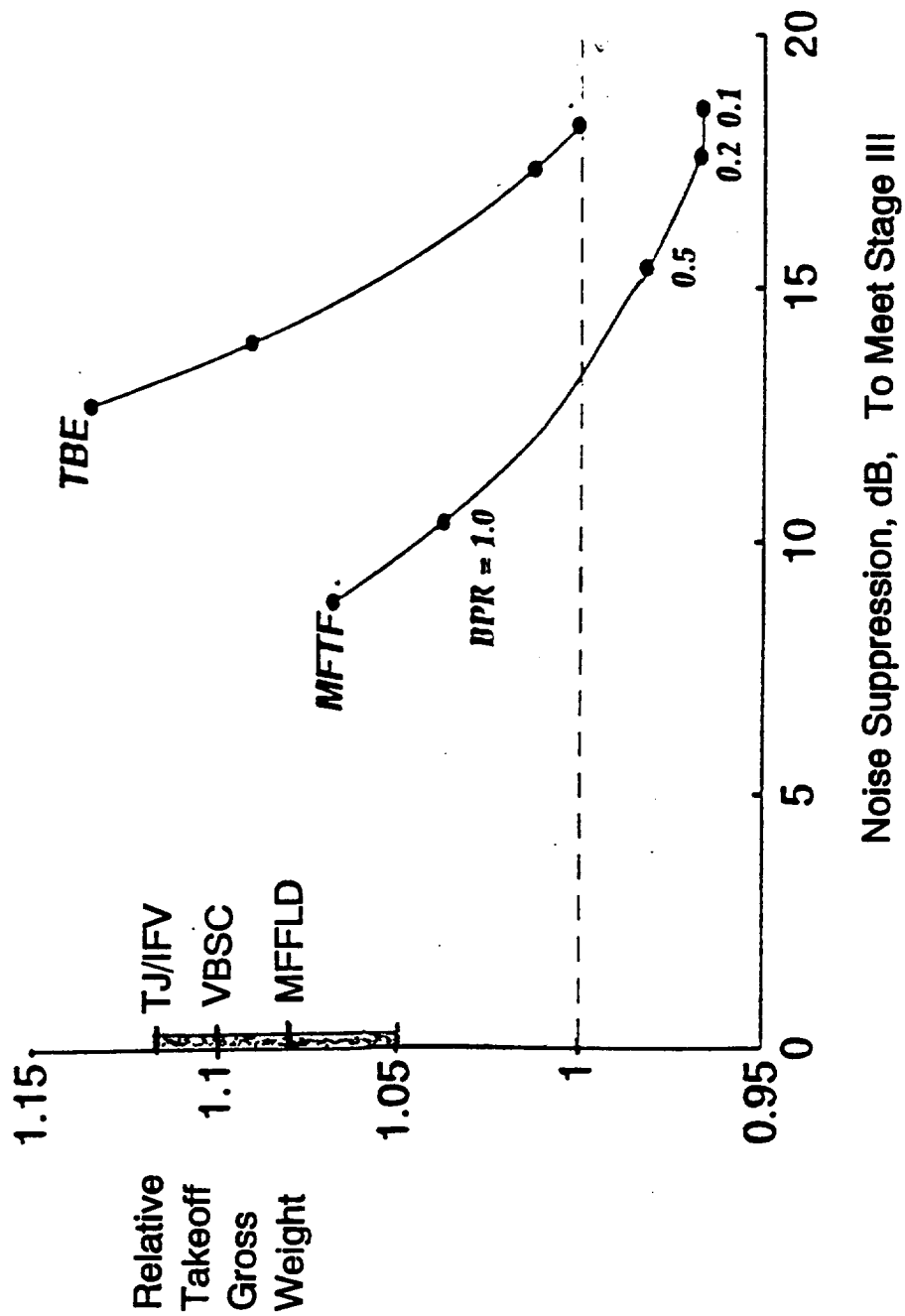


Figure 16

APPENDIX A

MIXING EFFECTIVENESS ANALYSIS FORMIXED FLOW TURBOFANS

The Problem

The aft end of a typical mixed flow turbofan engine is sketched in figure A1. The core exit flow, stream 1, meets the bypass duct flow, stream 2, in the mixer. The combined flows then enter the nozzle.

The intention of figure A1 is to illustrate that the mixing of the two flows can be incomplete. The nozzle must perform with some portion of the flow unmixed. In idealized flows, the sum of the gross thrusts of two separate flow streams is less than the gross thrust that would be produced by the mixed streams. Mixing effectiveness, E , is used to estimate the amount of gain in mixed flow thrust relative to separate flow thrust for conditions of partially mixed flows as in the following equation.

$$F_{GEST} = E(F_{GMI} - F_{GSI}) + F_{GSI} \quad (A1)$$

where F_{GEST} is the estimated thrust, F_{GMI} is the ideal mixed thrust, and F_{GSI} is the sum of the ideal separate flow thrusts. These elements of equation A1 are developed in the following discussion.

The relations developed in the following equations are familiar to specialists in the engine industry, where this approach to thrust correction for partially mixed nozzle flows has achieved general agreement and has been successfully applied. However, up to the present, the NEPP engine cycle analysis code has not included such thrust corrections for mixing effectiveness. The purpose of this appendix is to develop the background and rationale for this thrust correction and to stress the need for its incorporation in engine cycle performance analysis.

Background

For ideal isentropic nozzle expansion, the gross thrust can be shown to depend on total temperature, T , and total pressure, P ,

$$F_G = \dot{m} V_J = \dot{m} \sqrt{T} \sqrt{2Jg C_p \left[1 - \left(P / P_{amb} \right)^{(1-\gamma)/\gamma} \right]} = M \sqrt{T} K_P$$

where K_P depends on the total pressure, P , and the appropriate γ and C_p of the flow. M is the flow rate \dot{m} .

The ideal thrust of the separate streams (1 and 2) of figure A1 can be written as,

$$F_{GSI} = M_1 \sqrt{T_1} K_{P_1} + M_2 \sqrt{T_2} K_{P_2} \quad (A2)$$

If, however, the two streams are ideally mixed before the nozzle, the gross thrust of the mixed stream is,

$$F_{GMI} = (M_1 + M_2) \sqrt{T_{MX}} K_{P_{MX}} \quad (A3)$$

where T_{MX} is the mixed total temperature and $K_{P_{MX}}$ depends on the γ , C_p , and total pressure of the mixed stream.

Practical constraints on relative Mach number of the flow streams at the mixer entrance tend to limit the difference in total pressure of the two streams to less than 30%. Frequently, the total pressure difference is near zero. In a very simplified development, all K_P are considered equal, assuming nearly equal total pressures, g , and C_p . The ratio of ideal separate and mixed flow thrusts, f_1 , is then expressed as a function of M and T of the flows.

$$f_1 = \frac{F_{GSI}}{F_{GMI}} = \frac{M_1 \sqrt{T_1} + M_2 \sqrt{T_2}}{(M_1 + M_2) \sqrt{T_{MX}}}$$

(A4)

The mixed total temperature, T_{MX} , is based on a simple mass average of the flows, with equal C_p , such that,

$$T_{MX} = \frac{M_1 T_1 + M_2 T_2}{(M_1 + M_2)} \quad (A5)$$

Equation A4 can then be written, for this simple case, as,

$$f_1 = \frac{1 + \frac{M_2}{M_1} \sqrt{\frac{T_2}{T_1}}}{\sqrt{\left(1 + \frac{M_2}{M_1}\right) \left(1 + \frac{M_2 T_2}{M_1 T_1}\right)}} \quad (A6)$$

Figure A2 shows the relation between f_1 , M_2/M_1 , and T_2/T_1 given in equation 6. Note that equation 6 is an approximation based on ignoring differences in total pressure, C_p , and γ of the flow streams. The lowest stream temperature ratio shown in figure A2 is .25 since, for a wide range of mixed flow engines, the temperature ratio is only rarely less than .3 and is more often between .4 and .5. Mass flow ratios are essentially equivalent to the engine bypass ratio. Values of M_2/M_1 , are shown from .15 to 6.0. As seen in figure 2, a gross thrust difference of more than 5% is possible for M_2/M_1 of about 2.0 as temperature ratio varies from 1.0 to .25. As stated earlier, f_1 is never greater than 1.0 and is exactly 1.0 when $T_2/T_1=1$, regardless of M_2/M_1 .

Dividing through equation A1 by F_{GMI} results in a factor, C_E , which expresses the ratio of mixed flow gross thrusts that would apply when mixing effectiveness is introduced.

$$C_E = \frac{F_{GEST}}{F_{GMI}} = E \left(1 - \frac{F_{GSI}}{F_{GMI}} \right) + \frac{F_{GSI}}{F_{GMI}}$$

or

$$C_E = E(1 - f_1) + f_1 \quad (A7)$$

where f_1 was defined in equations A4 and A6.

In computer simulations of mixed flow engines, the realistic mixer will, in general, incorporate friction and losses in total pressure. This is especially true for multi-lobed forced mixers. However, such analysis models also assume total mixing of the streams. Therefore, to account for partially mixed flows in the nozzle, the computed gross thrust of the totally mixed flow can be adjusted by using C_E from equation A7. The calculated C_E is assumed to represent the proportion of gross thrust for partial mixing to that of completely mixed nozzle flow. The realistic mixer and nozzle flow calculations, complete with internal losses (e.g. ΔP and C_{te}), are used in evaluating the gross thrust for complete mixing, F_{GCOMP} . The adjusted gross thrust, F_{GADS} , due to mixing effectiveness is the product of F_{GCOMP} and the proportionality factor, C_E .

$$F_{GADJ} = C_E \times F_{GCOMP} \quad (A8)$$

Implementation

Equations A6, A7 and A8 have been implemented in the NEPP engine cycle analysis code by introducing them in the nozzle subroutine. They are used only when the nozzle is to be supplied with mixer exit flow which is partially mixed. Added inputs to the nozzle are needed. These are:

SPEC (13) Mixing effectiveness, E

SPEC (14) The component number of the mixer.

In the nozzle, the gross thrust is calculated in the usual way, depending on gas properties of the nozzle entrance flow. The mixer inlet flows and temperatures are used to calculate approximate f_1 from equation 6. The input effectiveness, E, is then used to calculate C_E from equation A7. The gross thrust is then adjusted by C_E as in equation A8.

Results

An example of their application of mixing effectiveness is shown in Table I(a) for a typical mixed flow turbofan (MFTF) with a sea level static bypass ratio of .937. Values of E and the resultant values of C_E , F_G , and F_N are given at two flight conditions, Mach 2.4 /60,000 ft. and sea level static. The ratio of ideal separate flow thrust to ideal mixed thrust, f_1 , from equation A6 is shown to be .9705 at Mach 2.4 and .9639 at sea level. A change in effectiveness, E , from 1 to 0 results in a change in gross thrust of about 3 percent at 2.4M or about 4 percent at sea level for the engine in Table I(a).

However, note that the overall change in net thrust at 2.4M is about 9 percent as E varies between 1 and 0, due to the ratio (~3:1) of gross to net thrust. At low speed conditions, such as the sls case, there is little or no ram drag and therefore changes in net thrust are the same as changes in gross thrust. The potential for large changes in net thrust (hence, changes in SFC) at high speed can make the proper selection of E important in assessing the performance of bypass engines in supersonic flight. Currently, industry experts have stated that an E of .8 can be used in nozzles behind multi-lobed forced mixers in which all of the bypass duct flow is assumed to mix with 70 to 80 percent of the core flow for engines with a moderate bypass ratio of about 1 or less. However, in engines with un-forced mixing, the E may be only about .4.

Table I(b) consists of data similar to that of I(a), except that the engine is an MFTF with a much smaller sea level static bypass ratio of .095. Here the f_1 and C_E values are much closer to 1.0, hence changes in F_G and F_N are much smaller as E is changed. The greater sensitivity of F_N to changes in E at 2.4 M is still present in Table I(b).

Potential for Improvement

The relation between C_E and f_1 is shown in figure A3. Note that C_E and f_1 are equal only when $E=0$, or when both are 1.0. In all cases for E greater than 0, the

factor C_E is closer to 1.0 than f_I implying that changes in gross thrust will be smaller than changes in f_I . In figure A3, f_I is only shown between .9 and 1.0 since, as indicated in figure A2, f_I is usually greater than .94.

The sensitivity of C_E and, therefore, computed gross thrust to changes or errors in E or f_I can be shown by differentiating equation A7.

$$dC_E = d f_I (1 - E) + dE (1 - f_I)$$

This derivative shows that any uncertainty in choice of E can cause an uncertainty in C_E , but the change in C_E may be less than 10% of the change in E , due to the factor $(1 - f_I)$. This implies that a highly accurate value of E is not necessary. In addition, an error in f_I , perhaps caused by the simplifying assumptions in equations A4, A5, and A6, will have a smaller effect on C_E because of the factor $(1 - E)$. However, this factor can be about .5, which could produce an error in C_E of half the error in f_I . At high flight speed, with a gross to net thrust ratio of about 3, this implies a potential error in net thrust (and SFC) of 1.5 times the error in f_I . More certainty in f_I could improve the certainty of the calculated net thrust.

As described earlier, equation A6 for f_I is based on simplifying assumptions of nearly equal total pressures, g , and C_P for the separate and mixed ideal flows. However, a more accurate value of f_I could be calculated which does not ignore differences in total pressure and gas properties for the flow streams. Referring to the basic definition of f_I ,

$$f_I \equiv F_{GSI} / F_{GMI}$$

the value of F_{GSI} could be calculated for the separate flow streams 1 and 2, each with pressure and temperature dependent gas properties and an isentropic nozzle. An ideal no-loss mixing of the streams could then be calculated for an accurate, but ideal, mixed total temperature and pressure and, hence, F_{GMI} .

Figure A4 compares f_I from the approximation of equation A6 with the "actual" f_I calculated as described above. The approximate values of f_I in figure A4 are the same as those in figure A2. The actual F_{GSI} and F_{GMI} are based on pressure and temperature dependent gas properties, ideal mixing, and ideal isentropic nozzles. Values of stream total temperature ratio T_2/T_1 range from 0.3 to 0.5, whereas mass flow ratio ranges from 0.5 to 3.0. The approximate values of f_I are systematically higher than the actual f_I , with a difference of about 2% when T_2/T_1 is 0.3. As mentioned earlier, this 2% difference in f_I may result in 3% errors in SFC based on net thrust at high ratios of gross to net thrust. However, in actual applications, low values of temperature ratio occur mostly at low flight speed, hence low ratios of gross/net thrust (near 1.0). At higher flight speeds, stream temperature ratios are 0.4 or greater, where the differences in f_I are smaller. Both of these factors tend to diminish the impact of uncertainty in f_I on net thrust.

The diamond symbols on figure A4 represent an improvement in the calculation of the approximate f_I of equation A6 by recognizing only the C_P differences between the streams 1 and 2. These values of f_I , while still approximate, seem to indicate a major improvement in the estimated f_I which could be less complicated to implement in a computer code. In this modification, the basic equation for gross thrust is re-written as,

$$F_G = M \sqrt{C_p T} k_p$$

An appropriate value of C_P for each stream is then introduced in equations A2 through A5. As a result, the terms T_2/T_1 of equation A6 are replaced by the terms $C_{P2}T_2/C_{P1}T_1$.

$$F_I = \frac{1 + \frac{M_2}{M_1} \sqrt{\frac{C_{P2}T_2}{C_{P1}T_1}}}{\sqrt{\left(1 + \frac{M_2}{M_1}\right) \left(1 + \frac{M_2}{M_1} \frac{C_{P2}T_2}{C_{P1}T_1}\right)}} \quad (A9)$$

The improved approximate values of f_1 in figure A4 would decrease the uncertainty in predicted gross thrust to about 1/2% or less. More importantly, net thrust uncertainties in high speed flight would be less than 1%.

Conclusions

The problem of gross thrust correction for nozzles with partially mixed/ unmixed flows has been addressed by employing mixing effectiveness, E . It has been shown that a simple factor, based only on stream temperature and flow ratios, can be used, with a given E , to adjust calculated gross thrust to reflect incompletely mixed flow in the nozzle. These changes have been incorporated in NNEP cycle analysis code, and example results were shown. An improvement in the approximate thrust correction factor was also presented which includes the C_P of each flow stream. This improved approximate method is recommended since it is easily implemented and can greatly reduce the uncertainty of calculated adjustments in gross and net thrusts.

MIXER EFFECTIVENESS ISSUE
AFT END OF TYPICAL MIXED FLOW TURBOFAN
THE NOZZLE FLOW MAY NOT BE TOTALLY MIXED

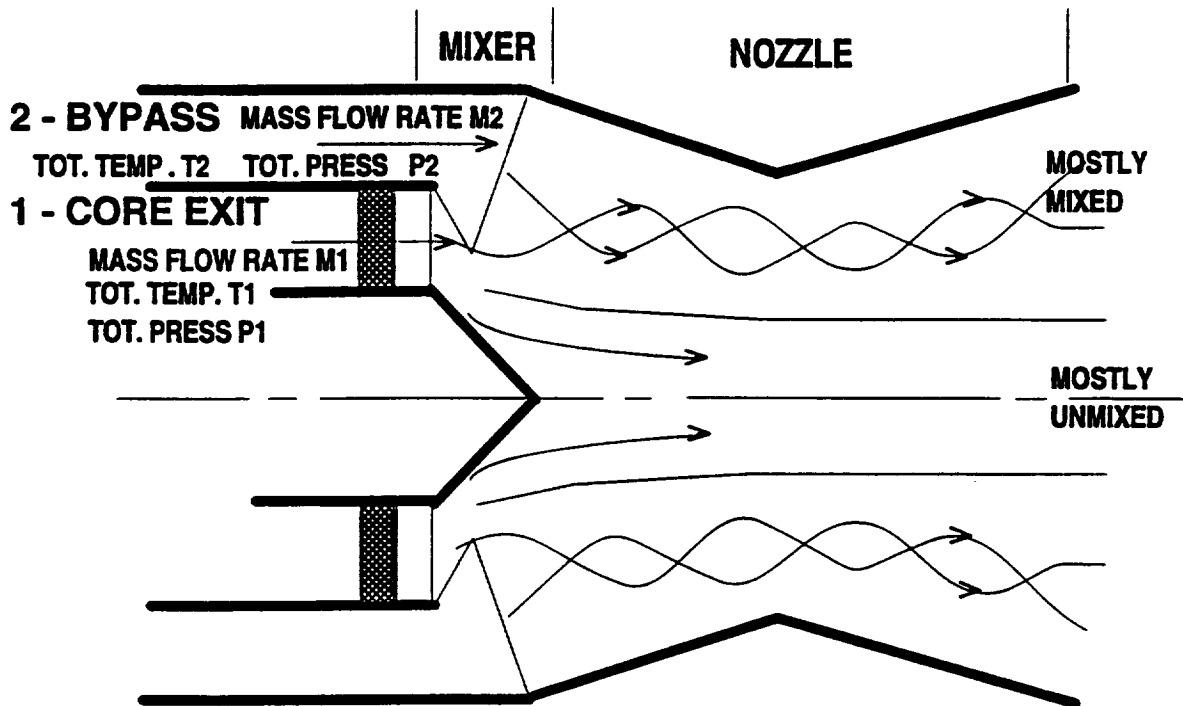


Figure A1

RATIO OF SEPARATE FLOW TO MIXED FLOW GROSS THRUST

IDEAL MIXING OF STREAMS M_1 AND M_2 WITH IDEAL NOZZLES
 APPROXIMATE ζ_I BASED ON EQUAL C_p AND γ .

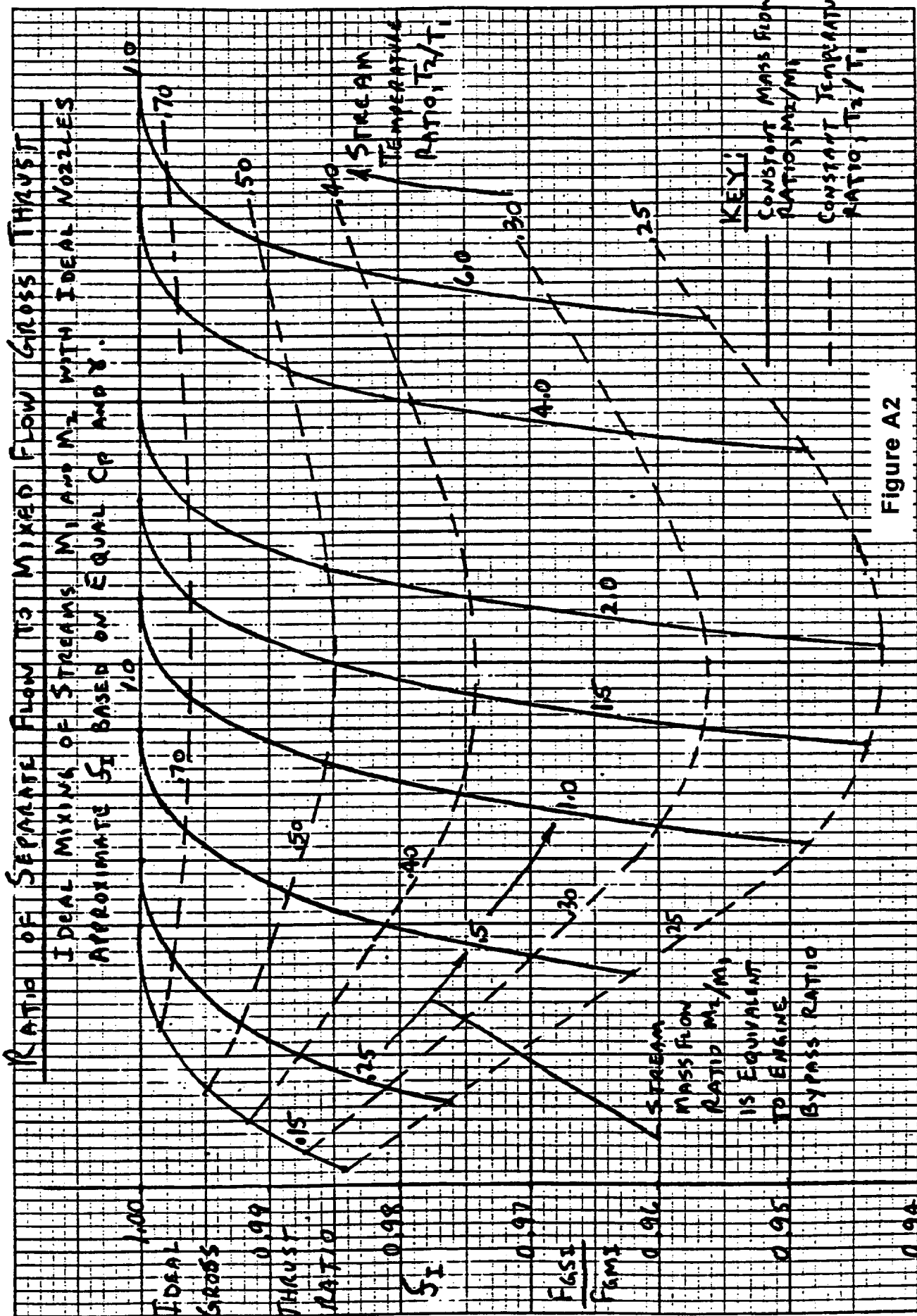


Figure A2

GROSS THRUST ADJUSTMENT DEPENDS ON S_I AND E

$$C_E = E(1 - S_I) + S_I$$

$$E = 1.0$$

Gross Thrust
Adjustment
Factor

C_E

$$E = .80$$

$$E = .60$$

$$E = .40$$

$$E = .20$$

$$E = .00$$

S_I , RATIO OF IDEAL SEPARATE AND MIXED GROSS THRUST

Figure A3

COMPARISON OF IDEAL GROSS THRUST RATIOS

IDEAL SEPARATE FLOW GROSS THRUST F_{GS1}

DIVIDED BY IDEAL MIXED FLOW GROSS THRUST F_{GM1}

APPROXIMATE S_I COMPARED WITH ACTUAL S_I

BASED ON CALCULATED F_{GS1} AND F_{GM1}

STREAM
TEMPERATURE
RATIO
 T_2/T_1

APPROXIMATE, SAME AS FIGURE 2,
USING EQUATION 6,

IMPROVED
APPROXIMATION
USING C_{p1} & C_{p2}
AND EQUATION 9.

ACTUAL, USING TEMPERATURE & PRESSURE DEPENDENT
 C_{p1} & C_{p2} WITH IDEAL MIXING AND IDEAL NOZZLES

1.00

IDEAL
GROSS
THRUST
RATIO 0.98

0.96

S_I

F_{GS1}
 F_{GM1}

0.94

0.92

0

1.0

2.0

3.0

STREAM MASS FLOW RATIO M_2/M_1

Figure A4

APPENDIX B

Glossary/Symbols - Main Body of Report

AIV -	Annular Inverting Valve
BPR -	By Pass Ratio
F_n/W_a -	Thrust per unit airflow - lb. thrust/lb. flow/sec
HPC -	High Pressure Compressor
HPT -	High Pressure Turbine
HSR -	High Speed Research
IGV -	Inlet Guide Vanes
IFV -	Invertor Flow Valve
K -	Ratio of total pressure in bypass duct to that in core at mixer
LPT -	Low Pressure Turbine
MFA -	Mass Flow Addition in the nozzle
MFFLD -	Mixed Flow FLadeD engine
MFTF -	Mixed Flow Turbofan
NEPP -	NASA Engine Performance Program
PR -	Pressure Ratio
PRF -	Pressure Ratio of Fan
RIT -	Rotor Inlet temperature - °R
RPM -	Revolutions Per Minute
SFC -	Specific Fuel Consumption - lb. fuel/sec/lb. thrust
T3 -	Compressor Outlet Temperature - °R
TBE -	Turbine Bypass Engine
TJ -	Turbojet
TTR -	Throttle Ratio - RIT_{max}/RIT
VBSC -	Variable Bypass Supercharged Core
V_j -	Jet Velocity - ft/sec
W_{ac2} -	Corrected flow at the high pressure compressor face

Glossary/Symbols for Appendix A

C_E -	Ratio of mixed flow gross thrusts when effectiveness is included
C_{fg} -	Gross thrust coefficient
C_p -	Specific heat coefficient at constant pressure - BTU/lb./°R
E -	Mixing effectiveness
F_G -	Gross Thrust - lb. force
F_{GADJ} -	Calculated gross thrust with effectiveness included - lb. force
F_{GCOMP} -	Calculated gross thrust with complete mixing - lb. force
F_{GEST} -	Estimate gross mixed thrust - lb. force
F_{GMI} -	Ideal gross mixed thrust - lb. force
F_{GSI} -	Sum of the ideal separate gross thrusts - lb. force
F_N -	Net thrust - lb. force
g -	gravitational acceleration - 32.174 ft/sec ²
J -	Conversion constant = 777.9 ft - lb _f /BTU
K_P -	Function of C_p , P and γ defined just before equation A2
M -	Mach number
\dot{m} -	Gas flowrate - lb _m /sec
P -	Pressure - lb _f /in ²
T -	Temperature - °R
T_{MX} -	Temperature of mixed streams - °R
V_j -	Jet velocity - ft/sec
γ -	Ratio of specific heats
f_i -	Ratio of ideal separate flow and mixed flow thrusts
ΔP -	Internal pressure loss in the nozzle

subscripts

I -	Ideal
1 -	Stream containing the core flow
2 -	Stream containing the bypass flow
MX -	Mixed stream
amb -	Ambient

REPORT DOCUMENTATION PAGE			Form Approved OMB No. 0704-0188	
Public reporting burden for this collection of information is estimated to average 1 hour per response, including the time for reviewing instructions, searching existing data sources, gathering and maintaining the data needed, and completing and reviewing the collection of information. Send comments regarding this burden estimate or any other aspect of this collection of information, including suggestions for reducing this burden, to Washington Headquarters Services, Directorate for Information Operations and Reports, 1215 Jefferson Davis Highway, Suite 1204, Arlington, VA 22202-4302, and to the Office of Management and Budget, Paperwork Reduction Project (0704-0188), Washington, DC 20503.				
1. AGENCY USE ONLY (Leave blank)		2. REPORT DATE April 2000		3. REPORT TYPE AND DATES COVERED Final Contractor Report
4. TITLE AND SUBTITLE Advanced Propulsion System Studies in High Speed Research			5. FUNDING NUMBERS WU-714-01-4A-00 NCC3-193	
6. AUTHOR(S) Charles L. Zola				
7. PERFORMING ORGANIZATION NAME(S) AND ADDRESS(ES) University of Toledo 2801 W. Bancroft Street Toledo, Ohio 43606-3328			8. PERFORMING ORGANIZATION REPORT NUMBER E-12233	
9. SPONSORING/MONITORING AGENCY NAME(S) AND ADDRESS(ES) National Aeronautics and Space Administration John H. Glenn Research Center at Lewis Field Cleveland, Ohio 44135-3191			10. SPONSORING/MONITORING AGENCY REPORT NUMBER NASA CR-2000-210035	
11. SUPPLEMENTARY NOTES Project Manager, Katherine Martin, High Speed Systems Office, NASA Glenn Research Center, organization code 2300, (216) 977-7122.				
12a. DISTRIBUTION/AVAILABILITY STATEMENT Unclassified - Unlimited Subject Categories: 05 and 07 This publication is available from the NASA Center for AeroSpace Information, (301) 621-0390.			12b. DISTRIBUTION CODE	
13. ABSTRACT (Maximum 200 words) Propulsion for acceptable supersonic passenger transport aircraft is primarily impacted by the very high jet noise characteristics of otherwise attractive engines. The mixed flow turbofan, when equipped with a special ejector nozzle seems to be the best candidate engine for this task of combining low jet noise with acceptable flight performance. Design, performance, and operation aspects of mixed flow turbofans are discussed. If the special silencing nozzle is too large, too heavy, or not as effective as expected, alternative concepts in mixed flow engines should be examined. Presented herein is a brief summary of efforts performed under cooperative agreement NCC3-193. Three alternative engine concepts, conceived during this study effort, are herein presented and their limitations and potentials are described. These three concepts intentionally avoid the use of special silencing nozzles and achieve low jet noise by airflow augmentation of the engine cycle.				
14. SUBJECT TERMS Propulsion; Turbofan engines; High Speed Civil Transport; SST			15. NUMBER OF PAGES 47	
			16. PRICE CODE A03	
17. SECURITY CLASSIFICATION OF REPORT Unclassified	18. SECURITY CLASSIFICATION OF THIS PAGE Unclassified	19. SECURITY CLASSIFICATION OF ABSTRACT Unclassified	20. LIMITATION OF ABSTRACT	

